



Baguet Tristan (Orcid ID: 0000-0002-1067-9374)

Descamps Benedicte (Orcid ID: 0000-0001-8879-1772)

**Radiosynthesis, *in vitro* and preliminary biological evaluation of [<sup>18</sup>F]FABABA, a novel ASCT-2 inhibitor based PET tracer.**

**Tristan Baguet<sup>1\*</sup>, Jakob Bouton<sup>2</sup>, Jonas Janssens<sup>2</sup>, Glenn Pauwelyn<sup>1</sup>, Jeroen Verhoeven<sup>1</sup>, Benedicte Descamps<sup>3</sup>, Serge Van Calenbergh<sup>2</sup>, Christian Vanhove<sup>3</sup>, Filip De Vos<sup>1</sup>.**

<sup>1</sup>Laboratory of Radiopharmacy, Ghent University, Ghent, Belgium

<sup>2</sup>Laboratory for Medicinal Chemistry, Ghent University, Ghent, Belgium

<sup>3</sup>IBiTech-MEDISIP, Department of Electronics and Information Systems, Ghent University, Ghent, Belgium

**\*Correspondence:**

Tristan Baguet

Email: [Tristan.baguet@ugent.be](mailto:Tristan.baguet@ugent.be)

**Number of words: 5962**

**Keywords: Positron emission tomography, oncology, glutamine, [<sup>18</sup>F]2-amino-4-((2-((3-fluorobenzyl)oxy)benzyl)(2-((3-(fluoromethyl)benzyl)oxy)benzyl)amino)butanoic acid, [<sup>18</sup>F]FABABA**

This article has been accepted for publication and undergone full peer review but has not been through the copyediting, typesetting, pagination and proofreading process which may lead to differences between this version and the Version of Record. Please cite this article as doi: 10.1002/jlcr.3863

## Abstract

**Introduction:** The metabolic alterations in tumors make it possible to visualize the latter by means of positron emission tomography, enabling diagnosis and providing metabolic information. The alanine serine cysteine transporter-2 (ASCT-2) is the main transporter of glutamine and is upregulated in several tumors. Therefore, a good positron emission tracer targeting this transport protein would have substantial value. Hence, the aim of this study is to develop a fluorine-18 labelled version of a V-9302 analogue, one of the most potent inhibitors of ASCT-2.

**Methods:** The precursor was labelled with fluorine-18 via a nucleophilic substitution of the corresponding benzylic bromide. The cold reference product was subjected to *in vitro* assays with [<sup>3</sup>H]glutamine in a PC-3 and F98 cell line to determine the affinity for both the human and rat alanine serine cysteine transporter-2. To evaluate the tracer potential dynamic  $\mu$ PET images were acquired in a mouse xenograft model for prostate cancer.

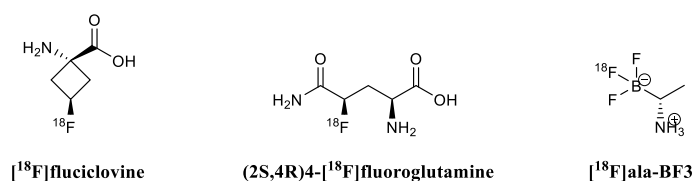
**Results:** The tracer could be synthesized with an overall non-decay corrected yield of  $3.66 \pm 1.90$  %. *In vitro* experiments show inhibitor constants  $K_i$  of 90  $\mu$ M and 125  $\mu$ M for the PC-3 and F98 cells, respectively. The experiments in the PC-3 xenograft demonstrate a low uptake in the tumor tissue.

**Conclusions:** We have successfully synthesized the radiotracer [<sup>18</sup>F]2-amino-4-((2-((3-fluorobenzyl)oxy)benzyl)(2-((3-(fluoromethyl)benzyl)oxy)benzyl)amino)butanoic acid. *In vitro* experiments show a good affinity for both the human and rat ASCT-2. However, the tracer suffers from poor *in vivo* tumor uptake in the PC-3 model. Briefly, we present the first fluorine-18 labelled derivative of compound V-9302, a promising novel ASCT-2 blocker used for inhibition of tumor growth.

## • Introduction

Cancer is characterized by genetic and epigenetic changes of individual cells leading to metabolic divergencies and unrestrained cell division<sup>1,2</sup>. Tumor can be classified based on their specific metabolic deviations. Attempts to exploit these changes has led to the development of anticancer drugs and imaging probes directed towards these altered molecular targets. Positron emission tomography (PET) is an imaging modality that uses probes labelled with radioactive isotopes. In oncology, PET tracers target the altered metabolic pathway, enabling the visualization of the tumor and providing metabolic information of the type of targeted metabolic pathway<sup>3</sup>.

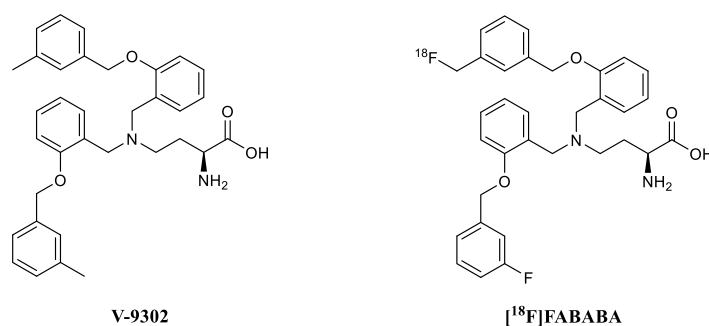
The alanine serine cysteine transporter-2 (ASCT-2) is the predominant transporter of glutamine in the human body. Considering the importance of glutamine in several types of tumor, research has been conducted towards the role of ASCT-2 in tumors. Upregulated levels of the transporter have been found in numerous tumors (e.g. colorectal cancer, pancreatic ductal carcinoma, breast cancer)<sup>4-6</sup>. In addition, it also appears to be a prognostic factor in some malignancies<sup>7,8</sup>. Developing radioactive probes to visualize ASCT-2 could therefore provide valuable information. Several attempts have been made to develop probes targeting ASCT-2, however none of them are selective or display good tumor uptake (see Scheme 1). [<sup>18</sup>F]fluciclovine is a radiotracer binding to ASCT-2 showing promising results with regard to prostate cancer imaging. However, this compound is not ASCT-2 selective as it also binds to large amino acid transporter-1 (LAT-1)<sup>9</sup>. (2*S*,4*R*)-4-[<sup>18</sup>F]fluoroglutamine, a glutamine-based PET tracer, targets ASCT-2 but suffers from *in vivo* defluorination<sup>10,11</sup>. A new ASCT-2 tracer, [<sup>18</sup>F]ala-BF<sub>3</sub>, shows potential but has only been preliminary tested<sup>12</sup>.



Scheme 1: Overview of ASCT-2 directed, fluorine-18 labelled, PET-radiotracers.

In 2016, Schulte et al. reported a class of compounds, the aryloxybenzyl aminobutanoic acids, which display the highest affinity for ASCT-2 reported to date, with IC<sub>50</sub>-values as low as 3 μM<sup>13</sup>. One of these compounds, V-9302, was further evaluated for its antitumor activity both *in vitro* and *in vivo*: V-9302 reduced cellular viability and increased cell death *in vitro*, and was capable of inhibiting tumor growth *in vivo*<sup>14</sup>. Given these promising results as an antitumor agent, we aimed at developing a fluorine-18 labelled version of a V-9302 analogue (see Scheme

2). In this analogue, both *meta*-methyl groups of the double 2-((3-methylbenzyl)oxy)-benzyl substituents on the nitrogen are replaced by a fluorine and fluoromethyl substituent, respectively, the latter containing the fluorine-18 label. A bromomethyl precursor would allow straightforward labelling. Cold reference product was subjected to *in vitro* [ $^3\text{H}$ ]glutamine uptake experiments to test affinity. The radioactive tracer was evaluated *in vivo* using a PC-3 xenograft mouse model to evaluate its imaging potential.

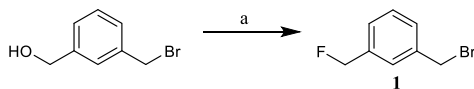


Scheme 2: Left: Chemical structure of V-9302, the lead molecule on which the new radiotracer is based upon. Right: Chemical structure of [ $^{18}\text{F}$ ]FABABA, modified on both *meta*-methyl groups, which are replaced with a fluorine and [ $^{18}\text{F}$ ]fluoromethyl group, respectively.

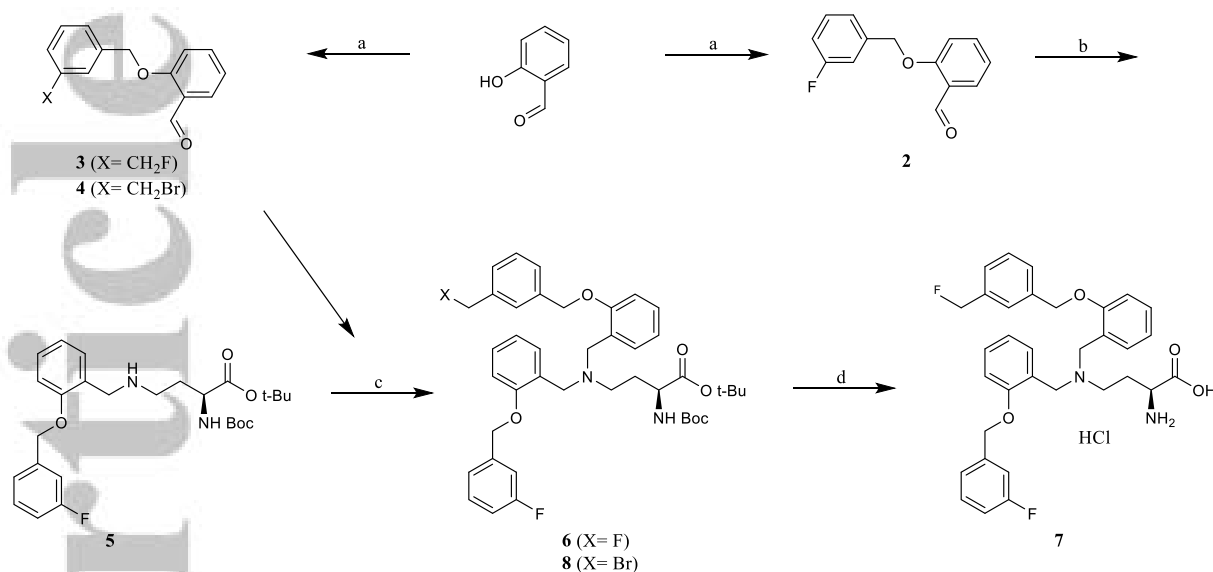
## • Results

### Chemistry

A five-step synthesis was developed to obtain cold reference product **7** (Scheme 4). The same synthesis was used to synthesize the precursor for radiolabeling. Fluorination of [3-(bromomethyl)phenyl]methanol with DAST afforded the requested 1-(bromomethyl)-3-(fluoromethyl)benzene (**1**) for the synthesis of intermediate **3** (Scheme 3). A Williamson ether synthesis was used to convert 2-hydroxybenzaldehyde to the ether products **2**, **3** and **4**. The yield of **4** was significantly lower than for **2** and **3**, due to formation of the double ether side-product with 1,3-bis(bromomethyl)benzene as a major side-product. Next, reductive amination of aldehyde **2** with (2*S*)-tert-butyl 4-amino-2-((tert-butoxycarbonyl)amino)butanoate hydrochloride according to Schulte et al. (2016) afforded **5**<sup>13</sup>. A small excess of *N*-Boc-*L*-2,4-diaminobutyric acid *tert*-butylester hydrochloride proved critical to avoid over-amination. A second reductive amination with benzaldehydes **3** and **4** resulted in compounds **6** and **8**. Compound **8** was then used as precursor for labelling with fluoride-18. Alternatively, deprotection of **6** with anhydrous HCl (4M in 1,4-dioxane) gave cold reference product **7**.



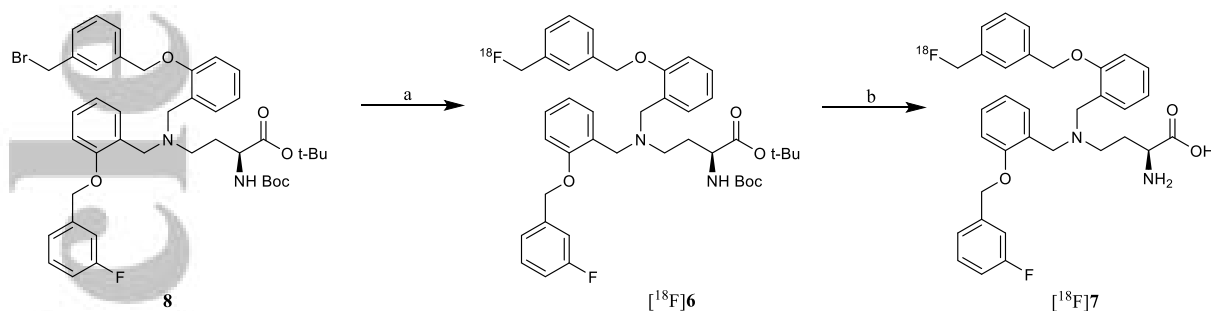
Scheme 3: Reagents and conditions: a) DAST, CH<sub>2</sub>Cl<sub>2</sub>, RT, 1 h, 61%.



Scheme 4: Reagents and conditions: a) appropriate benzylbromide, K<sub>2</sub>CO<sub>3</sub>, DMF, RT, 3 h, 28-100%; b) Boc-dab-OtBu, NaBH(OAc)<sub>3</sub>, CH<sub>2</sub>Cl<sub>2</sub>, RT, overnight, 53%; c) Aldehyde, NaBH(OAc)<sub>3</sub>, CH<sub>2</sub>Cl<sub>2</sub>, RT, overnight, 44-73%; d) 4M HCl in 1,4-dioxane, 40°C, 4 h, 100%.

### Radiochemistry

Synthesis of [<sup>18</sup>F]2-amino-4-((2-((3-fluorobenzyl)oxy)benzyl)(2-((3-(fluoromethyl)benzyl)oxy)benzyl)amino)butanoic acid ([<sup>18</sup>F]FABABA) (Scheme 5) was achieved with an overall non-decay corrected yield of  $3.66 \pm 1.90$  % and a total synthesis time of  $122 \pm 19$  minutes (n=3). Although high yields (>80%) of radiofluorination were observed, the total yield dropped significantly due to the challenging deprotection step which could not be improved. The combination of strong acidic conditions and high temperature is essential for the removal of protecting groups, but also results in partial degradation of the radiotracer. Co-injection with cold reference product on analytical HPLC confirmed the chemical purity ( $t_r$  [<sup>18</sup>F]FABABA = 18.5 min) (See Fig. S1 and Fig. S2). Quality control by means of analytical HPLC showed a radiochemical purity of >99%. The logD<sub>7.4</sub> was measured to be  $1.42 \pm 0.28$  (n=6).



Scheme 5: Radiochemical synthesis of  $[^{18}\text{F}]$ FABABA. Reagents and conditions: a)  $[^{18}\text{F}]$ F<sup>-</sup>, ACN, 120°C, 5 min; b) HCl (4 M in 1,4-dioxane), 90°C, 3.5 min, 3.66%.

### *In vitro experiments*

#### *In vitro stability*

Stability testing showed no degradation of  $[^{18}\text{F}]$ FABABA in its formulation. After 180 minutes only the mother compound was detected on analytical HPLC.

#### *Optimization of parameters for radiochemical labelling*

Optimization of the different reaction parameters showed inflection points for all three variables. Changing the solvent to acetonitrile increased the labelling yield significantly. Raising the temperature over 100°C turned out to be necessary for high yields. A total amount of 2 mg precursor is sufficient for good yields, while further increasing the precursor amount does not provide any additional gain in product. The ideal labeling parameters are acetonitrile as solvent, a reaction temperature of 120°C and at least 2 mg mass precursor. Graphical visualization of the influence of different parameters can be found in Figure 1.

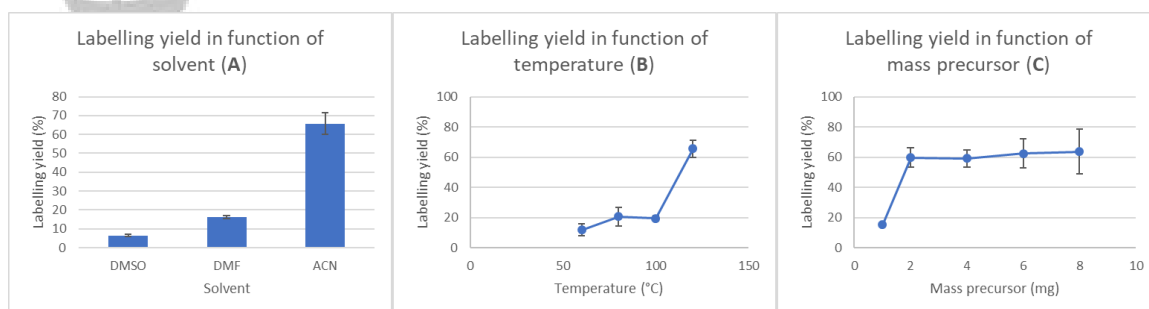


Figure 1: Optimization of the radiochemical synthesis yield of  $[^{18}\text{F}]$ FABABA. The optimization was done stepwise (one-parameter at a time, n=3). A: The labelling yield in

function of reaction solvent (DMSO, DMF and acetonitrile). **B:** The labelling yield in function of the temperature. The reaction temperatures tested were 60°C, 80°C, 100°C and 120°C. **C:** The labelling yield in function of the precursor mass.

#### ASCT-2 expression assay

Expression of ASCT-2 was confirmed on both the PC-3 and F98 cell lines (Figure 2**Error! Reference source not found.**). The PC-3 and F-98 cell line showed a median population of 12,056 (Specimen\_001-PC3 intra) and 28,585 (Specimen\_001-F98 intra), respectively. The median population of the negative control was 576 (Specimen\_001-PC3 surface) and 919 (Specimen\_001-F98 surface) for the surface staining of PC-3 and F98 cell line, respectively.

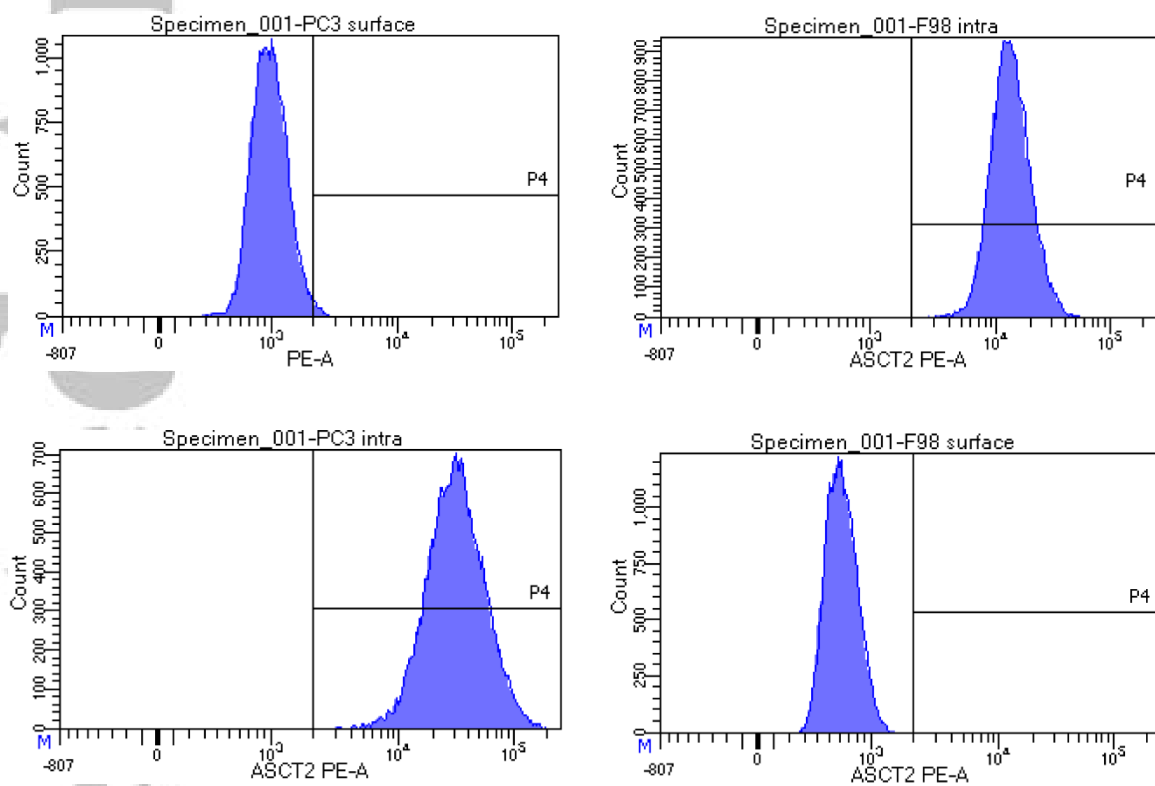


Figure 2: FACS measurement of ASCT-2 expression on PC-3 and F98 cells. Specimen\_001-PC3 intra and specimen\_001-F98 intra represents the intracellular staining of the PC-3 and F98 cells, respectively. Specimen\_001-PC3 surface figure and specimen\_001-F98 surface figure acts as a negative control and is the surface staining of the PC-3 and F98 cells, respectively.

Figure 3 represents the FACS analyses evaluating the ASCT-2 expression on the HEK-293 WT and HEK-293 KO cell lines as performed by the Creative Biogene company. The results show a positive expression population 66.3% and 0.454% for ASCT-2 on the HEK-293 WT and HEK-293 KO cell lines, respectively. The HEK-293 cell-iso and HEK-293 KO cell-iso, which



act as a negative control for the experiment, have a positive expression population of 0.643% and 0.151%, respectively.

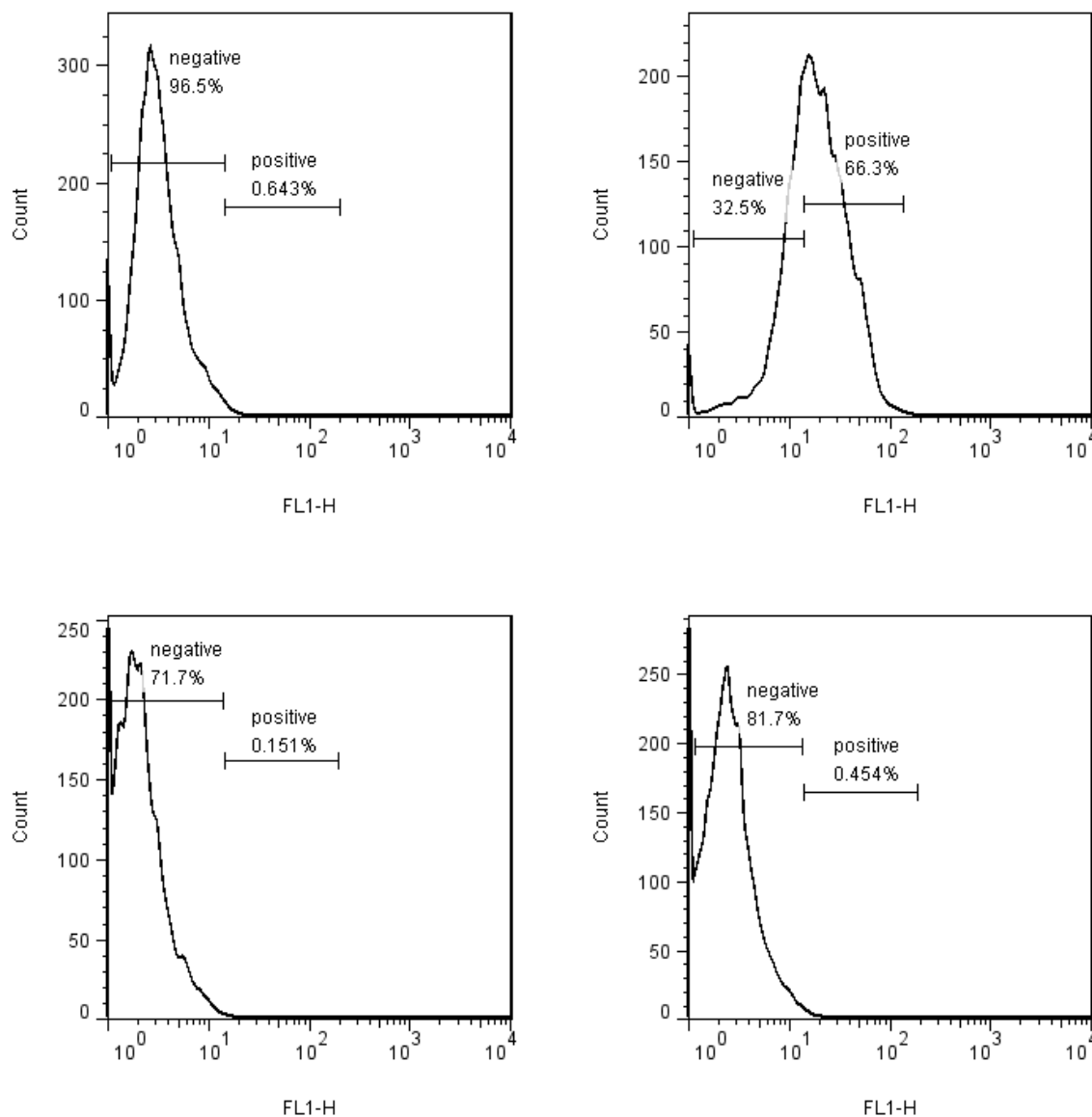


Figure 3: Top left: HEK-293 WT cell-iso; Top right: HEK-293 WT cell; Bottom left: HEK-293 KO cell Iso; Bottom Right: HEK-293 KO cell.

### *Concentration dependency*

The affinity of [ $^{19}\text{F}$ ]FABABA for ASCT-2 was determined in both rat F98 cells and human PC-3 cells. As a comparison, the affinity of V-9302 was also determined in the human PC-3 cell line. [ $^{19}\text{F}$ ]FABABA shows a  $K_i$  value of 90  $\mu\text{M}$  towards the glutamine transporter and inhibits glutamine uptake in a non-competitive manner (see Table 1). Compound V-9302

inhibits the glutamine transport in a comparative manner with a  $K_i$  value of  $150\mu\text{M}$ . In Figure 4 the Michaelis-Menten plots for the glutamine uptake can be found in both absence and presence of the inhibitor.

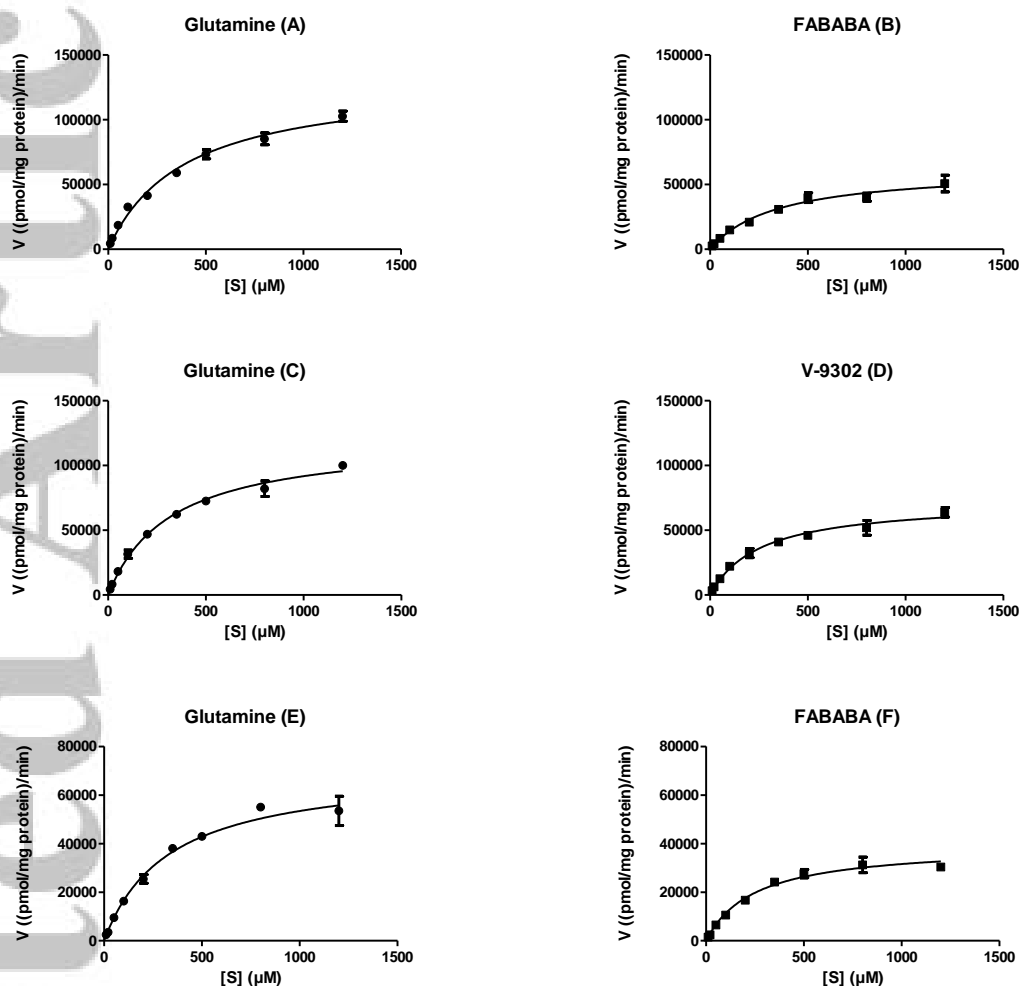


Figure 4: **A:** Concentration dependent uptake of  $[^3\text{H}]$ glutamine in PC-3 cells. **B:** Concentration dependent uptake of  $[^3\text{H}]$ glutamine in presence of FABABA in PC-3 cells. **C:** Concentration dependent uptake of  $[^3\text{H}]$ glutamine in PC-3 cells. **D:** Concentration dependent uptake of  $[^3\text{H}]$ glutamine in presence of V-9302 in PC-3 cells. **E:** Concentration dependent uptake of  $[^3\text{H}]$ glutamine in F98 cells. **F:** Concentration dependent uptake of  $[^3\text{H}]$ glutamine in presence of FABABA in F98 cells.

*Inhibition  $[^3\text{H}]-L$ -glutamine uptake in knock-out cell line:*

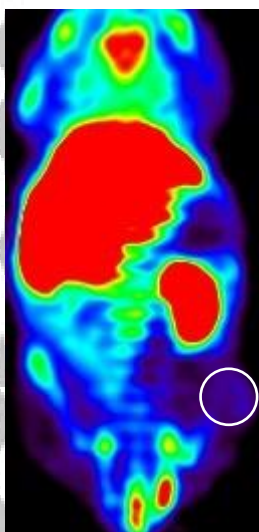
The selectivity of  $[^{19}\text{F}]$ FABABA towards the ASCT-2 cell line was assessed using a knock-out cell line.  $[^{19}\text{F}]$ FABABA shows a  $32 \pm 16\%$  and  $29 \pm 10\%$  inhibition of glutamine transport in ASCT-2 expressing F98 and HEK-293 WT cell lines, while in the ASCT-2 knock out cell line

[<sup>19</sup>F]FABABA inhibits transport with  $71 \pm 10\%$ . The inhibitor is therefore not selective for ASCT-2.

### *In vivo experiments*

*In vivo* experiments in PC-3 xenografts show that [<sup>18</sup>F]FABABA has only limited uptake in tumor tissue (see Figure 5). In both mice the tracer has a low standardized uptake value (SUV) and T/M ratio (see Table 2).

[<sup>18</sup>F]FABABA PET (A)



[<sup>18</sup>F]FABABA CT (B)



Figure 5:  $\mu$ PET acquisition of [<sup>18</sup>F]FABABA (A) and CT image (B) of the PC-3 xenograft tumor model (tumors delineated with a white circle).

### *Biodistribution study*

The results of the biodistribution of [<sup>18</sup>F]FABABA are shown in Table 3. Five minutes post-injection, the majority of radioactivity is found inside the liver tissue ( $28.87 \pm 2.82$  %ID/ g) and the blood pool ( $8.96 \pm 3.20$  %ID/ g). After twenty minutes, a large fraction remains in the liver ( $19.65 \pm 1.10$  %ID/ g) and the blood pool ( $6.11 \pm 1.03$  %ID/ g). Tumor uptake of the radiotracer is neglectable with only  $0.74 \pm 0.15$  %ID/ g found in tumor tissue. Fractions of the radioactivity was found in the muscle ( $0.62 \pm 0.19$  %ID/ g), brain ( $0.27 \pm 0.35$  %ID/ g), small intestine ( $1.07 \pm 0.46$  %ID/ g), bladder ( $1.71 \pm 0.73$  %ID/ g) and bone tissue ( $1.47 \pm 0.27$  %ID/ g).

## • Discussion

The unique tumor principle states every tumor possesses unique characteristics. Not only are there genetic and epigenetic differences between tumors, exogenous factors such as diet and lifestyle also contribute to uniqueness of neoplasms<sup>15</sup>. This heterogeneity makes it hard to estimate therapy effectiveness as each tumor will respond differently to the therapy. Grouping tumors to molecular (sub)classifications helps in predicting tumor behavior<sup>16,17</sup>. Collecting molecular information is therefore an important step in multimodality oncologic diagnosis and therapy. Positron emission tomography can provide such molecular information. Moreover, the more different kinds of tracers that are developed, the more information this modality can provide. In this study, we synthesized a novel PET-tracer targeting the alanine-serine-cysteine transporter-2. As the major transporter of the amino acid glutamine, we believe that imaging this transporter could provide valuable information in the metabolic mapping of the tumor.

A five-step synthesis was successfully used to gain access to the cold reference product. The precursor for fluorine-18 tagging was synthesized following the same scheme. To obtain an 18-fluorine derivative of compound V-9302, chemical adjustments to the structure had to be made. While doing this, the possibility to obtain a less lipophilic compound without impairing the pharmacological characteristics of V-9302 was explored. Changing the methyl-group to a fluorine was a non-invasive switch and was supported by the following two arguments. First, the LogP was computed in Chemdraw for V-9302 (6.52) and FABABA (5.84), which was advantageous for FABABA. Secondly, in the previous paper described by Schulte (2016)<sup>13</sup>, the incorporation of a fluorine directly on the arene altered the affinity in only a small manner. This trade-off seemed positive and therefore the methyl arm was chosen over the fluor arm. Radiochemical synthesis was successful, however only low non-decay corrected yields were obtained. Despite good labelling with fluorine-18, the deprotection step deteriorated the overall yield. Optimization of this step was not successful. The *in vitro* K<sub>i</sub> experiments showed that the FABABA compound has a moderate affinity for both the human and rat ASCT-2. The observed affinity in the PC-3 cell line (90 μM) is comparable to that of compound V-9302 (150 μM), on which FABABA was based upon. Moreover, Schulte et al. (2016) showed that comparable compounds also inhibited ASCT2-mediated glutamine uptake in human cells in a concentration-dependent fashion and reported IC<sub>50</sub> values ranging from 1.3 - 68.2 μM and from 7.2 - 141.7 μM, in rat and human cell lines, respectively<sup>13</sup>. A comparison of V-9302 and FABABA with regard to selectivity was not pursued in this manuscript. However, experiments using FABABA in the ASCT-2 knock-out cell line suggests the latter not being selective to ASCT-2 whereas literature on V-9302 does suggest ASCT-2 selectivity. This can be explained

to the above mentioned substitutions of methylgroups with fluorine and methylfluorine on the structure of V-9302. Despite the good affinities we observed *in vitro*, the *in vivo* experiments showed almost no uptake in the tumor tissue. Both the dynamic PET acquisitions and the biodistribution study demonstrate a slightly higher uptake in tumor tissue compared to muscle tissue. However, this is better explained by a very low uptake in muscle tissue rather than an elevated tumor uptake. As organs such as liver and intestines are immediately visible and dominate the uptake of the fluorine-18, we presume this radiotracer undergoes heavy metabolization (e.g., O-dealkylation, N-dealkylation, oxidation). This is supported by the results in the biodistribution study, where the radiotracer is primarily found in the liver tissue five minutes post-injection. In contrast, compound V-9302 that was described by Schulte et al. (2018) showed good inhibition of tumor growth<sup>14</sup>, which indicates tumor uptake. However, administration was at much higher dosage (75 mg/ kg) compared to the tracer amount we used. Moreover, kinetics of metabolization are hard to compare between the radiotracer and cold product used for treatment purposes. The functional groups, where metabolization is possible, are inherent to the compound and are necessary for good affinity, indicating that metabolic optimization for molecular imaging will be very challenging.

- **Conclusion**

[<sup>18</sup>F]FABABA could be synthesized, albeit with low overall yields. *In vitro* experiments show good affinity towards ASCT-2, comparable to the affinity of lead compound V-9302. However, the *in vivo* experiments show neglectable uptake in the tumor and demonstrate that the [<sup>18</sup>F]FABABA compound is not able in properly visualizing the PC-3 xenograft tumors. Further research should clarify the potential of [<sup>18</sup>F]FABABA in visualizing other tumor types. We hereby reported the first fluorine-18 labelled derivative of compound V-9302, a promising novel ASCT-2 blocker used for inhibition of tumor growth.

- **Material and methods**

### *General*

All reactions were performed under N<sub>2</sub> atmosphere. The chemicals used in these reactions were at least reagent grade, obtained from Sigma Aldrich (Bornem, Belgium), TCI Europe (Zwijndrecht, Belgium), Activate Scientific (Prien, Germany), Acros (Geel, Belgium) or ChemCollect (Wuppertal, Germany) and used as received. Solvents were at least HPLC-grade and were obtained from Chemlab (Zedelgem, Belgium). Chemical reactions were monitored on pre-coated TLC sheets (ALUGRAM® Xtra SIL G/UV<sub>254</sub>) under a wave length of 254 nm. Spots were visualized by spraying with either basic aqueous solution of KMnO<sub>4</sub> (1.0 g KMnO<sub>4</sub>, 2.0 g K<sub>2</sub>CO<sub>3</sub>, 100 mL H<sub>2</sub>O); 2,4-dinitrophenylhydrazine (12 g 2,4-DNP, 60 mL H<sub>2</sub>SO<sub>4</sub>, 80 mL H<sub>2</sub>O, 200 mL 95% EtOH) or ninhydrin (1.5g ninhydrin, 3.0 mL acetic acid, 100 mL EtOH) followed by subsequent charring. Purifications were done either by manual (Machery-Nagel Kieselgel 60 (63-200 μm)) or automated (Reveleris X2 (Grace)) flash chromatography. A mass spectrometer (Waters LCT Premier XE Time of Flight (TOF)), equipped with electrospray ionization (ESI) and modular Lockspray<sup>TM</sup> was used to obtain high resolution mass spectra. NMR spectra were recorded on a Varian Mercury-300BB (300 MHz) spectrometer.

### *Chemistry*

#### *General Procedure A (Williamson ether synthesis)*

Benzylic bromide (19.7 mmol, 1.2 eq) was dissolved in anhydrous DMF (85 mL; 5 mL/ mmol) in a flame-dried flask with stir bar under N<sub>2</sub> atmosphere. Salicylaldehyde (1.71 mL, 16.4 mmol) and K<sub>2</sub>CO<sub>3</sub> (5.65 g; 41.0 mmol; 2.5 eq) were added and the mixture was allowed to stir overnight at room temperature. The next day, the solvent was removed *in vacuo* and the residue was partitioned between CH<sub>2</sub>Cl<sub>2</sub> and H<sub>2</sub>O. The phases were separated, and the aqueous phase extracted twice more with CH<sub>2</sub>Cl<sub>2</sub>. The combined organic phases were dried over Na<sub>2</sub>SO<sub>4</sub> and concentrated *in vacuo*. The residue was purified by flash column chromatography (FCC).

### *1-(bromomethyl)-3-(fluoromethyl)benzene (1)*

(3-(bromomethyl)phenyl)methanol (1.00 g; 5.00 mmol) (Scheme 3) was dissolved in CH<sub>2</sub>Cl<sub>2</sub> (10 mL; 2 mL/ mmol) in a flame-dried flask and stirred for 10 min at 0°C. Diethylaminosulfur trifluoride (DAST, 0.66 mL, 5.00 mmol, 1 equivalent) was added dropwise, the reaction mixture was removed from the ice bath and was allowed to stir for 1 hour at room temperature. Upon disappearance of all starting material on TLC, the mixture was neutralized via dropwise addition of H<sub>2</sub>O (10 mL). Next, the compound was partitioned between H<sub>2</sub>O and CH<sub>2</sub>Cl<sub>2</sub>. The phases were separated, and the aqueous layer further extracted with CH<sub>2</sub>Cl<sub>2</sub> (2x). The combined organic phases were dried over Na<sub>2</sub>SO<sub>4</sub> and concentrated *in vacuo*. The residue was adsorbed on celite® and purified by automated column chromatography (0% EtOAc → 5% EtOAc in hexane) to afford **1** (0.613 g; 3.05 mmol) as a transparent liquid in 61% yield. R<sub>f</sub> 0.66 (10% EtOAc/ 90% Hex). <sup>1</sup>H NMR (300 MHz, CDCl<sub>3</sub>): δ 4.50 (s, 2H, CH<sub>2</sub>Br), 5.38 (d, *J*= 48 Hz, 2H, CH<sub>2</sub>F), 7.28-7.43 (m, 4H, H<sub>Phe</sub>). <sup>13</sup>C NMR (75 MHz, CDCl<sub>3</sub>): δ 32.98, 82.93, 85.17, 127.28, 127.35, 127.84, 127.93, 129.06, 129.12, 129.29, 129.34, 129.57, 136.80, 137.03, 138.25, 138.40. <sup>19</sup>F NMR (282 MHz, CDCl<sub>3</sub>): δ -208,75 (t, *J*= 47.9 Hz). Exact Mass: (ESI-MS) for C<sub>8</sub>H<sub>8</sub>BrF [M+H] found, non; calcd, 202.9872

### *2-((3-fluorobenzyl)oxy)benzaldehyde (2)*

Salicylaldehyde (1.71 mL; 16.4 mmol) and 1-(bromomethyl)-3-fluorobenzene (2.45 mL; 19.7 mmol) were coupled using procedure A. The product was purified by automated flash chromatography (4% EtOAc → 14% EtOAc in hexane) to afford **2** (3.51 g; 15.3 mmol) as a white powder in 93% yield. R<sub>f</sub> 0.36 (10% EtOAc/ 90% Hex). <sup>1</sup>H NMR (300 MHz, CDCl<sub>3</sub>): δ 5.19 (s, 2H, CH<sub>2</sub>-O), 7.00-7.24 (m, 5H, H<sub>Phe</sub>), 7.33-7.42 (m, 1H, H<sub>Phe</sub>), 7.50-7.57 (m, 1H, H<sub>Phe</sub>), 7.85-7.89 (m, 1H, H<sub>Phe</sub>), 10.57 (d, *J*= 0.7, 1H, CHO). <sup>13</sup>C NMR (75 MHz, CDCl<sub>3</sub>): δ 69.60, 69.64, 112.88, 113.94, 114.23, 115.03, 115.31, 121.26, 122.56, 122.60, 125.18, 128.66, 130.30, 130.40, 135.92, 138.61, 160.68, 189.51. <sup>19</sup>F NMR (282 MHz, CDCl<sub>3</sub>): δ [-112.40; -112.30] (m). Exact Mass: (ESI-MS) for C<sub>14</sub>H<sub>11</sub>FO<sub>2</sub> [M+H] found 231.0810, calcd, 231.0821

### *2-((3-(fluoromethyl)benzyl)oxy)benzaldehyde (3)*

Salicylaldehyde (0.258 mL; 2.48 mmol) and compound **1** (0.441 mL, 2.97 mmol) were coupled using procedure A. The product was purified by automated flash chromatography (5% EtOAc

→ 20% EtOAc in hexane) to afford **3** (0,606 g; 2.48 mmol) as a transparent liquid in quantitative yield.  $R_f$  0.67 (25% EtOAc/ 75% Hex).  $^1\text{H}$  NMR (300 MHz,  $\text{CDCl}_3$ ):  $\delta$  5.21 (s, 2H,  $\text{CH}_2\text{O}$ ), 5.42 (d,  $J=51$  Hz, 2H,  $\text{CH}_2\text{F}$ ), 7.02-7.09 (m, 2H,  $\text{H}_{\text{Phe}}$ ), 7.33-7.58 (m, 5H,  $\text{H}_{\text{Phe}}$ ), 7.85-7.89 (m, 1H,  $\text{H}_{\text{Phe}}$ ), 10.56 (d,  $J=0.73$  Hz, 1H, CHO).  $^{13}\text{C}$  NMR (75 MHz,  $\text{CDCl}_3$ ):  $\delta$  70.17, 83.14, 85.37, 112.94, 121.15, 125.18, 126.07, 126.13, 127.16, 127.28, 127.54, 127.57, 128.57, 129.06, 135.93, 136.62, 136.97, 160.88, 189.63.  $^{19}\text{F}$  NMR (282 MHz,  $\text{CDCl}_3$ ):  $\delta$  -208.15 (t,  $J=47.1$  Hz). Exact Mass: (ESI-MS) for  $\text{C}_{15}\text{H}_{14}\text{FO}_2$  [ $\text{M}+\text{H}$ ] found, 245.0984; calcd, 245.0978

#### 2-((3-(bromomethyl)benzyl)oxy)benzaldehyde (**4**)

Salicylaldehyde (1.71 mL; 16.4 mmol) and 1,3-bis(bromomethyl)benzene (5.20 g; 19.7 mmol) were coupled using procedure A. The product was purified by manual flash chromatography (5% EtOAc → 15% EtOAc in hexane) to afford **4** (1.40 g; 4.59 mmol) as a white powder in 28% yield.  $R_f$  0.38 (10% EtOAc/ 90% Hex).  $^1\text{H}$  NMR (300 MHz,  $\text{CDCl}_3$ ):  $\delta$  4.51 (s, 2H,  $\text{CH}_2\text{Br}$ ), 5.19 (s, 2H,  $\text{CH}_2\text{O}$ ), 7.02-7.09 (m, 2H,  $\text{H}_{\text{Phe}}$ ), 7.36-7.57 (m, 5H,  $\text{H}_{\text{Phe}}$ ), 7.84-7.89 (m, 1H,  $\text{H}_{\text{Phe}}$ ), 10.56 (d,  $J=0.7$  Hz, 1H, CHO).  $^{13}\text{C}$  NMR (75 MHz,  $\text{CDCl}_3$ ):  $\delta$  33.06, 70.08, 112.94, 121.17, 125.18, 127.26, 127.79, 128.59, 128.92, 129.24, 135.93, 136.83, 138.39, 160.78, 189.62. Exact Mass: (ESI-MS) for  $\text{C}_{15}\text{H}_{14}\text{BrO}_2$  [ $\text{M}+\text{H}$ ] found, 305.0327; calcd, 305.0177

#### Tert-butyl 2-((tert-butoxycarbonyl)amino)-4-((2-((3-fluorobenzyl)oxy)benzyl)amino)butanoate (**5**)

To a vial equipped with a magnetic stir bar, NBoc-L-2,4 diaminobutyric acid *tert*-butyl ester hydrochloride (2.98 g; 9.58 mmol) was dissolved in dry  $\text{CH}_2\text{Cl}_2$  (80 mL; 10 mL/ mmol). Compound **2** (2.10 g; 9.13 mmol) was added together with sodium triacetoxyborohydride (4.50 g; 21.2 mmol). The reaction was stirred at room temperature overnight. Upon completion, the reaction mixture is partitioned between  $\text{H}_2\text{O}$  and  $\text{CH}_2\text{Cl}_2$ , the phases separated, and the aqueous phase extracted with additional  $\text{CH}_2\text{Cl}_2$  (2X) and dried over anhydrous sodium sulfate. After concentration *in vacuo* the residue was purified by automated flash chromatography (40% EtOAc → 70% EtOAc in hexane). Compound **5** (2.36 g; 4.84 mmol) was obtained as a yellow oil in 53% yield.  $R_f$  0.19 (100% EtOAc).  $^1\text{H}$  NMR (300 MHz,  $\text{CDCl}_3$ ):  $\delta$  1.40 (s, 9H, *t*Bu), 1.42 (s, 9H, *t*Bu), 1.72-1.89 (m, 2H,  $\text{CH}_2\text{-CH}_2\text{-CH}$ ), 2.71-2.83 (m, 2H,  $\text{NH-CH}_2\text{-CH}_2$ ), 3.94 (dd,  $J_1=18.5$  Hz,  $J_2=13.1$  Hz, 2H,  $\text{CH}_2\text{-NH}$ ), 4.09-4.22 (m, 1H,  $\text{CH}_2\text{-CH-NH}$ ), 5.12 (s, 2H,



CH<sub>2</sub>O), 5.51-5.62 (m, 1H, NHBoc), 5.99 (s, 1H, CH<sub>2</sub>-NH-CH<sub>2</sub>), 7.86-7.25 (m, 6H, H<sub>Phe</sub>), 7.29-7.40 (m, 2H, H<sub>Phe</sub>). <sup>13</sup>C NMR (75 MHz, CDCl<sub>3</sub>): δ 27.90, 28.27, 31.41, 44.54, 47.84, 52.47, 69.29, 79.73, 82.05, 111.72, 113.92, 114.21, 114.77, 115.03, 121.18, 122.57, 122.62, 129.15, 130.21, 130.32, 130.72, 130.39, 139.51, 156.46, 161.33, 164.60, 171.39. <sup>19</sup>F (282 MHz, CDCl<sub>3</sub>): δ [-112.60; -112.90] (m). Exact Mass: (ESI-MS) for C<sub>27</sub>H<sub>38</sub>FN<sub>2</sub>O<sub>5</sub> [M+H] found 489.2766, calcd, 489.2765.

*Tert-butyl*2-((*tert*-butoxycarbonyl)amino)-4-((2-((3-fluorobenzyl)oxy)benzyl)(2-((3-(fluoromethyl)benzyl)oxy)benzyl)amino)butanoate (**6**)

To a flame-dried flask, with stir bar, was added compound **5** (400 mg; 0.82 mmol) dissolved in CH<sub>2</sub>Cl<sub>2</sub> (10 mL; 10 mL/mmol), compound **3** (0.209 mL; 0.86 mmol) and NaBH(OAc)<sub>3</sub> (608 mg; 2.87 mmol). The mixture was stirred overnight at room temperature under N<sub>2</sub> atmosphere. Upon completion of the reaction, the mixture was transferred to a separation funnel followed by addition of 10 mL H<sub>2</sub>O. The phases were separated, and the aqueous phase was extracted twice more with CH<sub>2</sub>Cl<sub>2</sub>. The combined organic layers were dried over Na<sub>2</sub>SO<sub>4</sub> and concentrated *in vacuo*. The residue was purified with flash chromatography (5% EtOAc in hexane +1% Et<sub>3</sub>N, isocratic). Compound **6** (0.429 g; 0.599 mmol) was obtained as a white oil with 73% yield. R<sub>f</sub> = 0,28 (10% EtOAc in hexane + 1%Et<sub>3</sub>N). <sup>1</sup>H NMR (300 MHz, CDCl<sub>3</sub>): δ 1.32 (s, 9H, *t*Bu), 1.42 (s, 9H, *t*Bu), 1.74-1.90 (m, 1H, CH<sub>2</sub>-CH<sub>2</sub>-CH), 1.93-2.09 (m, 1H, CH<sub>2</sub>-CH<sub>2</sub>-CH), 2.42-2.74 (m, 2H, N-CH<sub>2</sub>-CH<sub>2</sub>), 3.72 (dd, *J*<sub>1</sub>= 15 Hz, *J*<sub>2</sub>= 9Hz, 4H, CH<sub>2</sub>N), 4.04-4.18 (m, 1H, CH<sub>2</sub>-CH-NH), 5.06 (s, 2H, CH<sub>2</sub>O), 5.09 (s, 2H, CH<sub>2</sub>O), 5,37 (d, *J*= 47.7 Hz, 2H, CH<sub>2</sub>F), 5.72 (d, *J*= 6Hz, 1H, NH), 6.81-7.21 (m, 9Hz, H<sub>Phe</sub>), 7.27-7.53 (m, 7H, H<sub>Phe</sub>). <sup>13</sup>C NMR (75 MHz, CDCl<sub>3</sub>): δ 27.85, 28.39, 29.32, 50.68, 52.28, 53.41, 69.16, 69.73, 79.13, 81.27, 83.30, 85.50, 111.63, 111.72, 113.82, 114.09, 114.44, 114.73, 120.89, 121.00, 122.47, 122.50, 126.12, 126.19, 126.74, 126.82, 127.50, 127.54, 127.79, 127.81, 127.87, 128.85, 129.99, 130.10, 130.32, 136.42, 136.65, 137.88, 139.95, 140.05, 155.44, 156.49, 156.71, 161.30, 164.57, 171.70. <sup>19</sup>F NMR (282 MHz, CDCl<sub>3</sub>): δ [-112.90; -112.72] (m), -207.60 (t, *J*= 27.9 Hz). Exact Mass: (ESI-MS) for C<sub>42</sub>H<sub>51</sub>F<sub>2</sub>N<sub>2</sub>O<sub>6</sub> [M+H] found 717.3606, calcd, 717.3715.

*2-amino-4-((2-((3-fluorobenzyl)oxy)benzyl)(2-((3-(fluoromethyl)benzyl)oxy)benzyl)amino)butanoic acid (**7**)*

Compound **6** (230 mg; 0.32 mmol) was dissolved in HCl (4M in 1,4-dioxane, 5.0 mL) in a flame-dried flask. The mixture was stirred for 1 hour at 40°C under N<sub>2</sub>-atmosphere after which it was concentrated *in vacuo*. Pure compound **7** (0.32 mmol) was obtained as a white powder in quantitative yield. R<sub>f</sub> 0,37 (10% MeOH in CH<sub>2</sub>Cl<sub>2</sub>). <sup>1</sup>H NMR (300 MHz, DMSO-d<sub>6</sub>, 80°C): δ 4.31 (s, 4H, CH<sub>2</sub>N), 5.15 (d, 6.9 Hz, 4H, CH<sub>2</sub>O), 5.37 (d, *J* = 47.4 Hz, 2H, CH<sub>2</sub>F), 6.86-7.72 (m, 16H, H<sub>Phe</sub>). <sup>13</sup>C NMR (75 MHz, CDCl<sub>3</sub>) 24.83, 29.66, 50.38, 51.08, 52.80, 59.42, 61.66, 67.09, 69.62, 70.22, 83.23, 85.51, 112.33, 114.13, 114.85, 117.72, 121.64, 123.07, 126.57, 127.27, 127.97, 129.14, 130.47, 131.64, 133.78, 136.66, 139.11, 156.74, 156.98, 161.06, 164.32, 170.08. <sup>19</sup>F NMR (282 MHz, DMSO-D<sub>6</sub>, 80°C) δ [-113.06; -112.78] (m), -206.06 (t, *J* = 47.8 Hz). Exact Mass: (ESI-MS) for C<sub>33</sub>H<sub>35</sub>F<sub>2</sub>N<sub>2</sub>O<sub>4</sub> [M+H] found 561.2553, calcd, 561.2565.

*tert-butyl 4-((2-((3-(bromomethyl)benzyl)oxy)benzyl)(2-((3-fluorobenzyl)oxy)benzyl)amino)-2-((tert-butoxycarbonyl)amino)butanoate (8)*

In a flame-dried flask with stirbar, compound **5** (2.18g; 4.44 mmol) was dissolved in anhydrous CH<sub>2</sub>Cl<sub>2</sub> (80 mL; 20 mL/mmol). Compound **4** (1427 mg; 4.69 mmol) was added, followed by sodium triacetoxymethylborohydride (3.32 g; 15.7 mmol). The reaction was stirred for 24 h, followed by the addition of H<sub>2</sub>O and extraction with CH<sub>2</sub>Cl<sub>2</sub> (3x). The combined organic layers were washed with brine and dried over Na<sub>2</sub>SO<sub>4</sub>. The reaction mixture was concentrated *in vacuo* and purified by automated flash chromatography (10% EtOAc → 18 % EtOAc in hexane + 1% Et<sub>3</sub>N). Compound **8** (1.52 g; 1.95 mmol) was obtained as a transparent wax in 44% yield. R<sub>f</sub> 0.38 (10% EtOAc in hexane + 1% Et<sub>3</sub>N). <sup>1</sup>H NMR (300 MHz, CDCl<sub>3</sub>): δ 1.32 (s, 9H, *t*Bu), 1.41 (s, 9H, *t*Bu), 1.75-1.91 (m, 1H, CH<sub>2</sub>-CH<sub>2</sub>-CH), 1.93-2.06 (m, 1H, CH<sub>2</sub>-CH<sub>2</sub>-CH), 2.43-2.70 (m, 2H, N-CH<sub>2</sub>-CH<sub>2</sub>), 3.72 (dd, *J*<sub>1</sub>=15Hz, *J*<sub>2</sub>= 9Hz, 4H, CH<sub>2</sub>N), 4.03-4.15 (m, 1H, CH<sub>2</sub>-CH-NH), 4.47 (s, 2H, CH<sub>2</sub>Br), 5.06 (s, 4H, CH<sub>2</sub>O), 5.66-5.77 (m, 1H, NH), 6.80-7.03 (m, 5H, H<sub>Phe</sub>), 7.07-7.22 (m, 4H, H<sub>Phe</sub>), 7.27-7.54 (m, 7H, H<sub>Phe</sub>). <sup>13</sup>C NMR (75 MHz, CDCl<sub>3</sub>): δ 27.87, 28.39, 29.31, 33.32, 50.66, 52.28, 53.05, 53.39, 69.16, 69.67, 111.64, 111.75, 113.81, 114.07, 114.45, 114.74, 121.00, 122.51, 127.24, 127.79, 128.41, 129.02, 130.02, 130.11, 130.32, 138.05, 155.42, 156.42, 156.71, 161.30, 164.54, 171.69. <sup>19</sup>F NMR (300 MHz, CDCl<sub>3</sub>): δ -112.77 (s). Exact Mass: (ESI-MS) for C<sub>42</sub>H<sub>51</sub>BrFN<sub>2</sub>O<sub>6</sub> [M+H] found 777.2947, calcd, 777.2915

*Radiosynthesis of [<sup>18</sup>F]2-amino-4-((2-((3-fluorobenzyl)oxy)benzyl)(2-((3-(fluoromethyl)benzyl)oxy)benzyl)amino)butanoic acid ([<sup>18</sup>F]FABABA)*

Fluoride-18 (1.11 GBq) derived from cyclotron was trapped on a QMA light Sep-Pak cartridge (Water, Zellik, Belgium; preconditioned with 0.05 M K<sub>2</sub>CO<sub>3</sub> (10 mL) and ultrapure water (10 mL)) and eluted with cryptand-2.2.2./ K<sub>2</sub>CO<sub>3</sub> (1 mL of the following mixture: 9.4 mg cryptand-2.2.2. and 1.75 mg K<sub>2</sub>CO<sub>3</sub> dissolved in respectively acetonitrile (960 µL) and ultrapure water (40 µL)). The solvent was evaporated in a warm oil bath (100°C) under a gentle flow of N<sub>2</sub>-gas followed by two azeotropic drying steps after adding extra dry acetonitrile (1.0 mL). After placing the vial in an ice bath for 3 minutes, the reaction mixture (4.0 mg of compound **8** in 200 µL extra dry acetonitrile) was added and the vial was heated to 120°C for 5 minutes. Subsequently, the vial was placed in the ice bath for 3 minutes again, HCl (200 µL, 4.0 M in 1,4-dioxane) was added and the mixture was heated to 90°C for 3.5 minutes. PBS (100 µL) was added and the mixture was injected onto HPLC for purification. HPLC was done by using a C18 prep column (Atlantis T3 OBD prep column, 100Å, 10µM, 10mm x 250mm, 1/pkg, Waters), [<sup>18</sup>F]FABABA eluted after 15 minutes (mobile phase: acetonitrile/ammonium acetate (10 mM) in ultrapure water 45:55 (V:V); flowrate 6 mL/min). After elution, the collected fraction was diluted with PBS and trapped on a C18 Sep-Pak (preconditioned with acetonitrile (10 mL) and ultrapure water (10 mL)), washed with PBS (10 mL) and subsequently eluted with EtOH (1.0 mL). The EtOH was evaporated under a gentle flow of N<sub>2</sub>-gas (90°C) and the radiotracer was solubilized in an ethanol:PBS mixture (400 µL,10:90 (V:V)) to obtain the desired formulation.

The obtained radiotracer was subjected to quality control by means of analytical HPLC with radio and UV detection (205 nm; Waters) using a 1.0 mL/min flow and a Grace Alltima C18 (4.6 x 250 mm; 5 µm) column. Identification of the radiotracer was done by co-injection with compound **7** and comparing the retention time of the radiopeak to the UV-peak (18 min; mobile phase: gradient from 10 percent acetonitrile in ammonium acetate (10 mM) to 100 percent acetonitrile). logD<sub>7.4</sub> determination was done by adding 1 MBq radiotracer to a mixture of PBS water and n-octanol (1:1; V:V). Samples were vortexed and centrifuged (10 min; 1100 g) where after aliquots were taken from each layer which were measured in a NaI (TI) scintillation counter (Capintec; Ramsey, NJ, USA). logD<sub>7.4</sub> was calculated as the logarithm of the proportion of counts in the octanol and PBS layers.

#### *In vitro experiments*

#### *General information*

The cell lines were purchased from ATCC (PC-3, F98 and HEK-293 wild-type) and Creative Biogene (HEK-293 SLC1A5 knock-out cell line). RPMI medium enriched with 10% fetal calf serum, 1% L-glutamine and penicillin/streptomycin (50 U/ mL) was used to cultivate the PC-3 cells. The culture medium for the F98 cell line, HEK-293 wild-type (WT) and SLC1A5 knock-out (KO) cell line was Dulbecco's modified Eagle's medium (DMEM) enriched with 10% fetal calf serum, 1% L-glutamine and penicillin/streptomycin (50 U/ mL). All culture flasks were stored in an incubator set to 37°C and 5% CO<sub>2</sub> environment. Fluorescence-activated cell sorting (FACS) was used to evaluate the presence of ASCT-2 expression in PC-3 and F98 cell lines following the protocol described by De Munter et al.<sup>18</sup>. Both cell lines (100,000 cells/ 100 µL) were stained at their surface with a primary [rabbit ab; ASCT-2 (V501)] and secondary antibody [Fab2 (PE Conjugate); anti-rabbit IgG] against ASCT-2 as a negative control. The cells were fixed and permeabilized, followed by intracellular binding with the primary antibody. After binding of the primary antibody, the secondary antibody was added followed by an incubation period. All samples were analyzed at the end of the incubation period using the LSR II (BD Biosciences). The ASCT-2 KO cell line was engineered with CRISPR-CAS 9 using a HEK-293 WT cell line. Expression of ASCT-2 on both the HEK-203 WT and HEK-293 KO cell lines was also verified using fluorescence-activated cell sorting by Creative Biogene.

One day prior to the test, PC-3, F98, HEK-293 WT and ASCT-2 KO cells were seeded in 24-well plates (VWR, US) with a concentration of 175,000; 125,000; 175,000 and 175,000 cells per milliliter, respectively. To achieve good attachment of the HEK-293 WT and HEK-293 KO cells, the 24-well plates were coated prior to seeding: 300 µL of poly-D-lysine stock solution (0.1 mg/ mL) was added to each well and the plates were dried for 30 minutes until all solvent was removed. Upon removal of the solvent the plates were ready for cell attachment. A HEPES+ buffer (pH 7.4; 100 mM NaCl (Sigma Aldrich, Belgium), 2 mM KCl (Sigma Aldrich, Belgium), 1 mM MgCl<sub>2</sub> (VWR, US), 1 mM CaCl<sub>2</sub> (VWR, US), 10 mM Hepes (Sigma Aldrich, Belgium), 5 mM Tris (VWR, US), 1 g/ L glucose (VWR, US) and 1 g/ L Bovine Serum Albumin (Sigma Aldrich, Belgium)) was used to perform the [<sup>3</sup>H]glutamine uptake studies. The desired concentration series were made from a glutamine stock concentration (43.8 mg/ 30mL HEPES+). To each stock solution a total of 111 kBq/ mL [<sup>3</sup>H]-L-glutamine (Perkin Elmer, Massachusetts) was added. Concentration series containing [<sup>19</sup>F]FABABA were made next to the reference glutamine concentration series. The experiments were started by aspirating the medium and washing all wells with HEPES+ twice. After removal of HEPES+, test solution

(250  $\mu\text{L}$ ) was added, and the plates were incubated for 5 minutes at 37°C. After 5 minutes uptake was stopped by placing the plates on ice and adding ice cold PBS + BSA (1 mL, 1 g/100 mL). After removal of PBS +BSA, the wells were washed twice with ice cold PBS (2 mL) and cells were lysed by adding 0.1 M NaOH (250  $\mu\text{L}$ ) (VWR, US) and placing the plates on a shaker. Aliquots of 150  $\mu\text{L}$  were pipetted out of each well into a scintillation bottle (Perkin Elmer, Massachusetts, USA) and 5 mL of scintillation cocktail (Ultima Gold, Perkin Elmer, Massachusetts, USA) was added. Samples were measured with an automated scintillation counter (TriCarb 2900 TR; Perkin Elmer, Massachusetts, USA). Aliquots of 25  $\mu\text{L}$  cell lysis were subjected to the bicinchoninic acid assay (BCA) (ThermoFisher Scientific) to correct for protein density.

*Concentration dependency:* The uptake of [ $^3\text{H}$ ]-L-glutamine was tested in PC-3 human cells and F98 rat cells in absence of cold reference product and was compared to the uptake in the presence of cold reference products. Additionally, the uptake of [ $^3\text{H}$ ]-L-glutamine in PC-3 cells was also evaluated in the presence of compound V-9302. The glutamine stock solution used ranged from 10  $\mu\text{M}$  to 1200  $\mu\text{M}$ . Michaelis-Menten parameters were obtained by plotting the data of the liquid scintillation counter via non-linear regression in GraphPad prism v5.01 (GraphPad software, San Diego, CA, USA).  $K_m$  (values in absence of cold product) and  $K_{m,app}$  (apparent values in presence of cold product) data were used to calculate the  $K_i$  values according to the formula:  $V_{max, app} = \frac{V_{max}}{1 + \frac{[I]}{K_i}}$ , with [I] being the concentration of inhibitor.

*Inhibition [ $^3\text{H}$ ]-L-glutamine uptake in knock-out cell line:* To evaluate the selectivity of the radiotracer to ASCT-2, the inhibition of the [ $^3\text{H}$ ]-L-glutamine uptake in absence of ASCT-2 was measured in a knock-out cell line. The cells were incubated with 250  $\mu\text{L}$  50  $\mu\text{M}$  [ $^3\text{H}$ ]-L-glutamine/glutamine in absence and presence of compound **8** for 5 minutes at 37°C. The inhibition of glutamine uptake in HEK-293 KO was compared to glutamine inhibition in ASCT-2 expressing HEK-293 WT and F98 cells which was evaluated using the same protocol.

#### *In vitro evaluation of stability in formulation*

The stability of [ $^{18}\text{F}$ ]FABABA was evaluated in its formulation. After radiosynthesis the radiotracer formulation was incubated at 37°C for 30, 70, 120 and 180 minutes. At the indicated time points aliquots were taken (7 MBq) and analyzed by analytical HPLC (method cfr QC of [ $^{18}\text{F}$ ]FABABA).

#### *Optimization of parameters for radiochemical labelling*

The reaction parameters of the radiofluorination were optimized. Solvent, reaction temperature and mass precursor were altered one variable at a time. DMF, DMSO and acetonitrile were tested as reaction solvents. The different reaction temperatures were 60°C, 80°C, 100°C and 120°C. The concentration of precursor solution tested were 2 mg/ 200 µL; 4 mg/ 200 µL; 6 mg/ 200 µL; 8 mg/ 200µL extra dry acetonitrile. Radiochemical labelling yields were determined by TLC analysis.

*In vivo evaluation of [<sup>18</sup>F]2-amino-4-((2-((3-fluorobenzyl)oxy)benzyl)(2-((3-(fluoromethyl)benzyl)oxy)benzyl)amino)butanoic acid*

The Ghent University Ethical Committee on Animal Experiments approved the *in vivo* evaluation of the tracer in a PC-3 xenograft model prior to the start of the study, which was performed according to the appropriate guidelines and regulations (ECD 17/08). The xenografts were obtained by inoculating male swiss nu/nu mice with PC-3 tumor cells. At the day of inoculation, the PC-3 cells were harvested and suspended in non-enriched RPMI medium to obtain a  $5 \times 10^7$  cells/mL cell suspension. The mice (n=2) were injected with  $5 \times 10^6$  cells (+ 0.1 mL Matrigel®) in the right flank at the age of 8 weeks; one week later, the left flank was inoculated with  $5 \times 10^6$  cells (+ 0.1 mL Matrigel®). Tumor growth was followed with manual caliper measurements. During animal experiments, food and water were provided *ad libitum*. Dynamic µPET scans were acquired seven weeks post-inoculation and animals were fasted minimal six hours prior to imaging. Anesthesia was induced with 5.0% isoflurane (V:V in O<sub>2</sub>) and maintained with 2.0% until the end of the experiment. After intravenous injection of 18.5 MBq radiotracer in the lateral tail vein, dynamic PET acquisitions of 1 hour were performed on a FLEX Triumph II small animal PET/CT-scanner (PET field of view: 7.5 cm axial; 1.2 mm spatial resolution; TriFoil Imaging). Upon completion of the PET-scan an additional computed tomography (CT) scan was performed for anatomical correlation purposes. The resulting PET data were obtained in list mode and reconstructed iteratively (50 iterations) in frames of one minute the first twenty-five minutes and frames of five minutes for the following thirty-five minutes. PET and CT images were aligned using the AMIDE (Source Forge Media, La Jolla, CA, USA) software<sup>19</sup>. Region of interests (ROI) were drawn manually around the tumor and leg muscle as comparison tissue. Tumor-to-muscle (T/M) ratios were calculated and standard uptake values (SUV) were determined according to the following formula:

$$SUV = \text{Radioactivity in ROI (MBq/ml)} / \text{injected activity (MBq)} \times \text{body weight (g)}$$

### *Biodistribution study*

The distribution of the [<sup>18</sup>F]FABABA to the different organs of PC-3 inoculated mice was evaluated by means of a biodistribution study. The PC-3 xenograft model was set up as discussed above. Seven weeks post-inoculation, 5.0 MBq of radiotracer was injected intravenously via the lateral tail vein. At the indicated time points (5 min and 20 min post-injection) the mice were euthanized by cervical dislocation (n=3 for each time point). Blood was extracted via cardiac puncture and the organs were removed during dissection. To avoid any interference of adhering blood, all organs were rinsed with water. Subsequent weighing of the samples and counting of the radioactive signal provided the uptake in the organs expressed as percentage injected dose per gram of tissue (%ID/ g) ± SD.

#### • **List of abbreviations**

ASCT-2: Alanine serine cysteine transporter-2

CT: Computed tomography

DAST: Diethylaminosulfur trifluoride

DMEM: Dulbecco's modified Eagle's medium

DMF: Dimethylformamide

DMSO: Dimethylsulfoxide

[<sup>18</sup>F]FABABA: [<sup>18</sup>F]2-amino-4-((2-((3-fluorobenzyl)oxy)benzyl)(2-((3-(fluoromethyl)benzyl)oxy)benzyl)amino)butanoic acid

KO: Knock-out

LAT1: Large amino acid transporter-1

PBS: Phosphate buffered saline

PET: Positron emission tomography

ROI: Region of interest

SUV: Standardized uptake value

T/M: Tumor-to-muscle

- **Conflict of Interest**

The authors declare that the research was conducted in the absence of any commercial or financial relationships that could be construed as a potential conflict of interest.

- **Authors' contribution**

Conceptualization: TB JB JJ GP JV BD CV FDV

Data curation: TB JB JJGP JV BD CV

Formal analysis: TB JB JJ GP

Investigation: TB JB JJ GP JV

Methodology: TB BD SVC CV FDV

Project administration: SVC CV FDV

Resources: CV FDV

Software: TB JB JJ GP JV

Supervision: SCV CV FDV

Validation: TB GP

Visualization: TB

Writing - original draft: TB GP JV

Writing - review & editing: TB JB JJ GP JV BD SVC CV FDV

Tristan Baguet: TB; Jakob Bouton: JB, Jonas Janssens: JJ; Glenn Pauwelyn: GP; Jeroen Verhoeven: JV; Benedicte Descamps: BD; Serge Van Calenbergh: SVC, Christian Vanhove: CV; Filip De Vos: FDV



## • References

1. Hanahan D, Weinberg RA. The hallmarks of cancer. *Cell*. 2000;100(1):57-70. doi:10.1016/s0092-8674(00)81683-9
2. Greaves M. Cancer causation: The Darwinian downside of past success? *Lancet Oncol*. 2002;3(4):244-251. doi:10.1016/S1470-2045(02)00716-7
3. Lewis DY, Soloviev D, Brindle KM. Imaging of tumor metabolism using positron emission tomography (PET). *Cancer J*. 2015;21(2):129-136. doi:10.1007/978-3-319-42118-6\_8
4. Huang F, Zhao Y, Zhao J, et al. Upregulated SLC1A5 promotes cell growth and survival in colorectal cancer. 2014;7(9):6006-6014.
5. Kaira K, Sunose Y, Arakawa K, et al. Clinicopathological significance of ASC amino acid transporter-2 expression in pancreatic ductal carcinoma. 2015:234-243. doi:10.1111/his.12464
6. Kim S, Jung WH, Koo JS. The expression of glutamine-metabolism-related proteins in breast phyllodes tumors. 2013:2683-2689. doi:10.1007/s13277-013-0819-7
7. Toyoda M, Kaira K, Ohshima Y, et al. Prognostic significance of amino-acid transporter expression ( LAT1 , ASCT2 , and xCT ) in surgically resected tongue cancer. *Br J Cancer*. 2014;110(10):2506-2513. doi:10.1038/bjc.2014.178
8. Shimizu K, Kaira K, Tomizawa Y, et al. ASC amino-acid transporter 2 ( ASCT2 ) as a novel prognostic marker in non-small cell lung cancer. *Br J Cancer*. 2014;110(8):2030-2039. doi:10.1038/bjc.2014.88
9. Oka S, Okudaira H, Yoshida Y, Schuster DM, Goodman MM, Shirakami Y. Transport mechanisms of trans-1-amino-3-fluoro[1- <sup>14</sup>C]cyclobutanecarboxylic acid in prostate cancer cells. *Nucl Med Biol*. 2012;39(1):109-119. doi:10.1016/j.nucmedbio.2011.06.008
10. Qu W, Zha Z, Ploessl K, et al. Synthesis of optically pure 4-fluoro-glutamines as potential metabolic imaging agents for tumors. *J Am Chem Soc*. 2011;133(4):1122-1133. doi:10.1021/ja109203d
11. Venneti S, Dunphy MP, Zhang H, et al. Glutamine-based PET imaging facilitates

- enhanced metabolic evaluation of gliomas in vivo. *Sci Transl Med*. 2015;7(274). doi:10.1126/scitranslmed.aaa1009
12. Lui H, Han Y, Li J, et al. 18F-Alanine Derivative Serves as an ASCT2 Marker for Cancer Imaging. *Mol Pharm*. 2018;15(3):947-954. doi:10.1021/acs.molpharmaceut.7b00884.
  13. Schulte ML, Khodadadi AB, Cuthbertson ML, Smith JA, Manning HC. 2-Amino-4-bis(aryloxybenzyl)aminobutanoic acids: A novel scaffold for inhibition of ASCT2-mediated glutamine transport Dedicated to the memory of Eric S. Dawson, Ph.D. *Bioorganic Med Chem Lett*. 2016;26(3):1044-1047. doi:10.1016/j.bmcl.2015.12.031
  14. Schulte ML, Fu A, Zhao P, et al. Pharmacological blockade of ASCT2-dependent glutamine transport leads to antitumor efficacy in preclinical models. *Nat Med*. 2018;24(2):194-202. doi:10.1038/nm.4464
  15. Ogino S, Fuchs CS, Giovannucci E. How many molecular subtypes? Implications of the unique tumor principle in personalized medicine. *Expert Rev Mol Diagn*. 2012;12(6):621-628. doi:10.1586/erm.12.46.
  16. Ogino S, Goel A. Molecular classification and correlates in colorectal cancer. *J Mol Diagnostics*. 2008;10(1):13-27. doi:10.2353/jmoldx.2008.070082
  17. Ogino S, Chan AT, Fuchs CS, Giovannucci E. Molecular pathological epidemiology of colorectal neoplasia: An emerging transdisciplinary and interdisciplinary field. *Gut*. 2011;60(3):397-411. doi:10.1136/gut.2010.217182
  18. De Munter S, Ingels J, Goetgeluk G, et al. Nanobody based dual specific CARs. *Int J Mol Sci*. 2018;19(2):1-11. doi:10.3390/ijms19020403
  19. Loening AM, Gambhir SS. AMIDE: A Free Software Tool for Multimodality Medical Image Analysis. *Mol Imaging*. 2003;2(3):131-137. doi:10.1162/153535003322556877

Table 1: Affinity constant  $K_i$  for FABABA in human PC-3 cells and rat F98 cells.

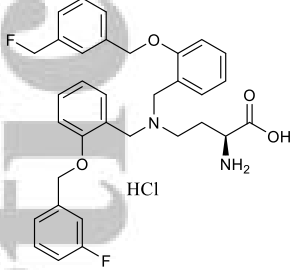
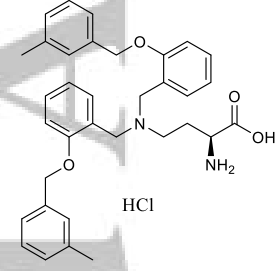
Compound	$K_i$ value PC-3 ( $\mu\text{M}$ )	$K_i$ value F98 ( $\mu\text{M}$ )
<p data-bbox="327 331 462 365"><b>FABABA</b></p> 	90	125
<p data-bbox="343 734 446 768"><b>V-9302</b></p> 	150	Not determined.

Table 2: Semiquantitative values of [18F]FABABA uptake in PC-3 xenograft. Mean tumor-to-muscle (T/M<sub>mean</sub>) ratios and mean standardized uptake values (SUV<sub>mean</sub>) are given for two mice.

	Mouse 1	Mouse 2
T/M <sub>mean</sub>	1.23	1.20
SUV <sub>mean</sub>	0.10	0.07

Table 3: Tissue uptake of [<sup>18</sup>F]FABABA in various organs and the blood of Swiss nu/nu male mice at 5- and 20-minutes post-injection. Values are expressed as % ID/ g of tissue ± SD (n=3).

Organ	[ <sup>18</sup> F]FABABA	
	%ID/ g 5 min post-injection	%ID/ g 20 min post-injection
Blood	8.96 ± 3.20	6.11 ± 1.03
Tumor	0.091 ± 0.070	0.74 ± 0.15
Muscle	0.15 ± 0.17	0.62 ± 0.19
Brain	-0.01 ± 0.23	0.27 ± 0.35
Skin	0.55 ± 0.24	1.38 ± 0.18
Fat	0.08 ± 0.14	0.69 ± 0.36
Liver	28.87 ± 2.82	19.65 ± 1.10
Spleen	0.98 ± 0.34	1.13 ± 0.10
Lung	2.48 ± 0.91	2.50 ± 0.20
Kidney	3.80 ± 0.86	4.00 ± 0.29
Stomach	0.74 ± 0.32	0.63 ± 0.41
Small intestine	0.53 ± 0.35	1.07 ± 0.46
Large intestine	0.22 ± 0.19	0.19 ± 0.08
Bladder	-0.16 ± 0.47	1.71 ± 0.73
Bone	0.52 ± 0.33	1.47 ± 0.27
Heart	2.17 ± 0.53	1.87 ± 0.13